

TEMPORAL ADAPTIVE MULTIGRID CORRECTION METHOD FOR TRANSIENT NONLINEAR NODAL CALCULATIONS

Ku Young Chung and Chang Hyo Kim

Seoul National University
San 56-1 Shinlim-Dong Kwanak-Gu Seoul, Korea
niro90@snu.ac.kr ; kchoy@snu.ac.kr

ABSTRACT

A temporal adaptive multigrid correction method is developed as a way to speed up the transient nonlinear nodal calculations. The method incorporates the step-doubling scheme based on coarse grid residual equation into the three-grid correction scheme (3GCS) on the modified W cycle. The computational efficiency of the method is examined in terms of the NEACRP PWR rod ejection benchmark problem solutions. It is shown that the step-doubling algorithm using the coarse grid residual equation can predict the per-step temporal truncation error as accurately as the conventional one that is based on the fine grid residual equation and therefore it is very effective for reducing the computation overload of the conventional step doubling calculations by the fine grid residual equations. It is also shown that the temporal adaptive 3GCS can improve the convergence of the iterative solution to the kinetics benchmark problem by about 2~4 times.

Key Words: computational efficiency, transient nonlinear nodal calculation, temporal adaptive multigrid correction method, W-cycle, NEACRP PWR rod ejection benchmark problem.

1. INTRODUCTION

To improve the computational efficiency of transient nodal calculations, we previously presented a three-grid correction scheme (3CGS) as an acceleration method for the linear equation solver[1]. To further improve the transient nodal computational efficiency, we here incorporate the step-doubling method[2] utilizing the coarse grid equation as an adaptive temporal step control algorithm and BILU3D[3] preconditioner into the 3CGS and present the computational effectiveness of the resulting temporal adaptive multigrid correction scheme in comparison with the popular acceleration methods like the preconditioned BICGSTAB[4] available for the transient nodal neutronics calculations.

The time step size control algorithms are customarily employed to reduce the computational time of the transient neutronics calculations. Because the temporal differencing method for the transient neutron diffusion equation is associated with the temporal truncation error dependent on the time step size during the course of the transient, it is important to provide a robust method of determining it adaptively in order to obtain the solution of the desired uniform accuracy every time step. The two most popular variable time step algorithms currently in use are the step-doubling technique [2] and inverse period method [5]. The inverse period method boasts of the simplicity in its algorithm but has a shortfall not to monitor directly the truncation error [6]. We

adopted here a second-derivative-based step-doubling method [2] because it can monitor temporal truncation error directly and thus achieve the desired fidelity of the transient solution. As discussed in reference 6, however, the step-doubling method requires additional calculations to predict the temporal truncation error at each time step, and this additional calculation can cost about 50% overhead of the computing time. As a way to overcome this disadvantage, reference 2 suggests simplified additional calculations by using the norm of linear system matrix. As another way to reduce the overhead, we suggest here using the coarse grid linear system of equations which comprise a part of the system equations to be solved in the multigrid correction scheme.

In the following, we present the 3GCS and step-doubling method based on the coarse grid system of equations. To validate the suggested method, we perform the temporal adaptive 3GCS calculations for the transient solutions to the OECD/NEACRP PWR rod ejection benchmark problems [7]. The computational efficiency of the adaptive 3GCS scheme is discussed in comparison with other numerical schemes examined for the problem.

2. THREE-GRID CORRECTION SCHEME AND ADATIVE TIME STEP CONTROL

2.1. Transient Nonlinear Nodal Method

The transient nonlinear nodal method is designed to solve the following nodal neutron balance relations for the 3D rectangular node designated by the superscript m [8];

$$\begin{aligned} \frac{1}{v_g} \frac{d\Phi_g^m}{dt} = & \frac{1}{k_{eff}} \left(\chi_{pg} \sum_{g'=1}^2 (1-\beta) \Sigma_{fg'}^m \Phi_{g'}^m + \chi_{dg} \sum_{d=1}^D \lambda_d C_d^m \right) \\ & + \sum_{g'=1}^2 \Sigma_{g'g}^m \Phi_{g'}^m - \sum_{u=x,y,z} \frac{1}{h_u^m} (J_{gur}^m - J_{gul}^m) - \Sigma_{tg}^m \Phi_g^m \end{aligned} \quad (1)$$

and

$$\frac{dC_d^m}{dt} = \frac{1}{k_{eff}} \sum_{g'=1}^2 v_{dg'd} \Sigma_{fg'}^m \Phi_{g'}^m - \lambda_d C_d^m. \quad (2)$$

In the nonlinear nodal method, J_{gus}^m are related to Φ_g^m by [9]

$$J_{gus}^m = -D_{gus}^m (\Phi_{gus}^m - \Phi_g^m) - \tilde{D}_{gus}^m (\Phi_{gus}^m + \Phi_g^m) \quad (3)$$

where Φ_{gus}^m is the node average flux of the adjacent node in direct contact with the node m at left (s=l) or right side (s=r) in the u direction. D_{gus}^m is the coupling coefficient from the first order finite difference approximation for J_{gus}^m . \tilde{D}_{gus}^m is the corrective coupling coefficient that is to be updated by obtaining J_{gus}^m through two-node solution of well-known transverse integrated

one-dimensional diffusion equation. Substitution of Eq. (3) into Eq. (1) results in the nodal coarse mesh finite difference (CMFD) equation for the unknown nodal fluxes. A fully implicit time integration of the CMFD equation at time step n can lead to a linear system of equations that can be put into

$$\mathbf{A}_f^{(n)} \Phi_f^{(n)} = \mathbf{b}_f^{(n)}. \tag{4}$$

The subscript "f" denotes fine-grid system parameters. The 3-dimensional (3D), 4 node-per-assembly (N/A) is taken here as the fine grid in the 3GCS. Our aim is to solve Eq. (4) in the shortest possible computation time.

2.2. Coarse Grid Equations and Operators for 3GCS

To design the 3GCS we must define restriction and prolongation operators and also obtain the coarse grid equations. The 3GCS utilizes the two coarse grid equations corresponding to 3D 1N/A and 2D 1N/A grids, as displayed in Fig. 1. The subscripts "c1" and "c2" designate the 3D 1N/A and 2D 1N/A grid parameters, respectively. The restriction and the prolongation operators are used to transform the solution vector of one system of equations into that of another.

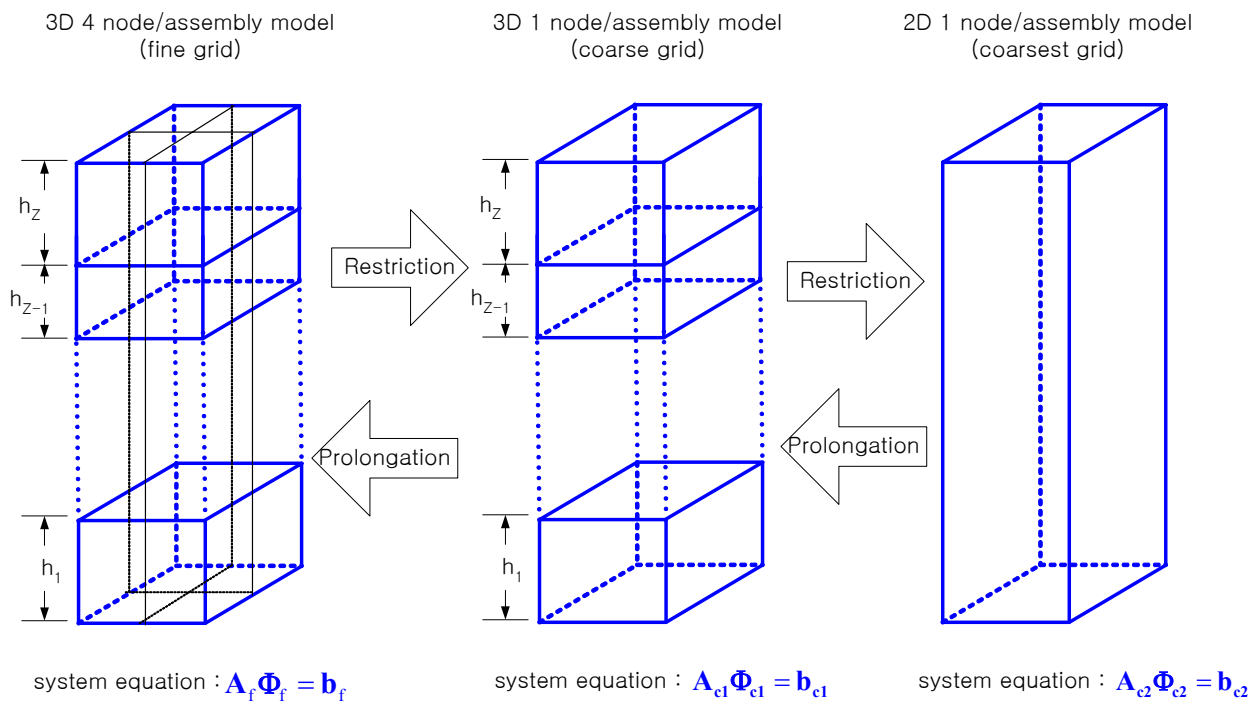


Figure 1. 3D 4N/A, 3D 1N/A, and 2D 1N/A grid structures

The restriction operation is a procedure to obtain the node-average flux of a coarse grid node that comprise the several fine-grid nodes from the fine-grid solution. Because the volume averaging procedure is used here, the restriction operators are defined as

$$\mathbf{R}_{f \rightarrow c1} = \begin{bmatrix} \ddots & & & & \mathbf{O} \\ & \left(\frac{1}{4} & \frac{1}{4} & \frac{1}{4} & \frac{1}{4} \right) & \\ & & & & \\ \mathbf{O} & & & & \ddots \end{bmatrix} \quad (5)$$

and

$$\mathbf{R}_{c1 \rightarrow c2} = \begin{bmatrix} \mathbf{R}_1 & & & & \\ & \mathbf{R}_2 & & & \\ & & \ddots & & \\ & & & \mathbf{R}_{N_R-1} & \\ & & & & \mathbf{R}_{N_R} \end{bmatrix} \quad (6)$$

where

$$\mathbf{R}_1 = \mathbf{R}_2 = \dots = \mathbf{R}_i = \dots = \mathbf{R}_{N_R} = \begin{bmatrix} w_1 & w_2 & \dots & w_{N_z} \end{bmatrix},$$

$$w_j = \frac{\text{volume of } j\text{-th coarse node in assembly}}{\text{volume of assembly}}. \quad (7)$$

Using the above restriction operators, one can get readily the coarse-grid flux vectors by

$$\Phi_{c1}^{(n)} = \mathbf{R}_{f \rightarrow c1} \Phi_f^{(n)} \quad (8)$$

and

$$\Phi_{c2}^{(n)} = \mathbf{R}_{c1 \rightarrow c2} \Phi_{c1}^{(n)}. \quad (9)$$

The prolongation operation is interpreted as the inverse procedure of restriction operation. In the conventional multigrid methods in which prolongation operators are derived from the interpolation principle[10], the prolongation operator is often referred to as the interpolation operator. Because of the coarse-grid structures adopted here, 3D 1N/A and 2D 1N/A, however, the interpolation procedure cannot be applied directly to the prolongation operation. Instead, we define the prolongation operators as follows;

$$\mathbf{P}_{c1 \rightarrow f}^{(n)} = \begin{bmatrix} \ddots & & & & \mathbf{O} \\ & \frac{1}{\Phi_{m,c1}^{(n-1)}} \begin{pmatrix} \Phi_{4m-3,f}^{(n-1)} \\ \Phi_{4m-2,f}^{(n-1)} \\ \Phi_{4m-1,f}^{(n-1)} \\ \Phi_{4m,f}^{(n-1)} \end{pmatrix} & & & \\ & & & & \\ \mathbf{O} & & & & \ddots \end{bmatrix} \quad (10)$$

and

$$\mathbf{P}_{c2 \rightarrow c1}^{(n)} = \begin{bmatrix} \mathbf{P}_1 & & & & \\ & \mathbf{P}_2 & & & \\ & & \ddots & & \\ & & & \mathbf{P}_{N_R-1} & \\ & & & & \mathbf{P}_{N_R} \end{bmatrix} \quad (11)$$

where

$$\mathbf{P}_i = \begin{bmatrix} p_{i,1} \\ p_{i,2} \\ \vdots \\ p_{i,N_Z} \end{bmatrix}; \quad p_{i,j} = \frac{\bar{\phi}_{(i,j),c1}^{(n-1)}}{\bar{\phi}_{(i),c2}^{(n-1)}} \quad (i=1, \dots, N_R, j=1, \dots, N_Z). \quad (12)$$

Note that these operators are obtained under the assumption that the fine-grid flux distribution does not change much during coarse grid correction procedure. The fine grid flux is then obtained from the coarse grid flux by

$$\Phi_{c1}^{(n)} = \mathbf{P}_{c2 \rightarrow c1}^{(n)} \Phi_{c2}^{(n)} \quad (13)$$

and

$$\Phi_f^{(n)} = \mathbf{P}_{c1 \rightarrow f}^{(n)} \Phi_{c1}^{(n)}. \quad (14)$$

The two coarse grid equations can be derived straightforwardly from Eq. (4) by using restriction and prolongation operators. To show this, let's multiply Eq.(4) by restriction operator to get

$$\mathbf{R}_{f \rightarrow c1} \mathbf{A}_f^{(n)} \Phi_f^{(n)} = \mathbf{R}_{f \rightarrow c1} \mathbf{b}_f^{(n)}. \quad (15)$$

Substitution of Eq. (14) into Eq (15) results in

$$\mathbf{R}_{f \rightarrow c1} \mathbf{A}_f^{(n)} \mathbf{P}_{c1 \rightarrow f}^{(n)} \Phi_{c1}^{(n)} = \mathbf{R}_{f \rightarrow c1} \mathbf{b}_f^{(n)} \quad \text{or} \quad \mathbf{A}_{c1}^{(n)} \Phi_{c1}^{(n)} = \mathbf{b}_{c1}^{(n)} \quad (16)$$

where

$$\mathbf{A}_{c1}^{(n)} = \mathbf{R}_{f \rightarrow c1} \mathbf{A}_f^{(n)} \mathbf{P}_{c1 \rightarrow f}^{(n)}, \quad \mathbf{b}_{c1}^{(n)} = \mathbf{R}_{f \rightarrow c1} \mathbf{b}_f^{(n)}. \quad (17)$$

Eq. (16) is the linear system of equations on “c1” coarse-grid. The similar procedure can produce c2 grid system equation,

$$\mathbf{A}_{c2}^{(n)} = \mathbf{R}_{c1 \rightarrow c2} \mathbf{A}_{c1}^{(n)} \mathbf{P}_{c2 \rightarrow c1}^{(n)}. \quad (18)$$

2.3. Modified W-cycle

Fig. 2 displays the basic idea of two-grid correction algorithm by which one corrects the fine grid error term with solution to coarse grid residual equation. Suppose that one has obtained an approximate p -th iterative solution, $\Phi_f^{(p)}$, to fine grid equation $\mathbf{A}_f \Phi_f = \mathbf{b}_f$. The fine grid error $\mathbf{e}_f^{(p)} (= \Phi_f - \Phi_f^{(p)})$ satisfies fine grid residual equation $\mathbf{A}_f \mathbf{e}_f^{(p)} = \mathbf{r}_f^{(p)}$ with fine grid residual $\mathbf{r}_f^{(p)} (= \mathbf{b}_f - \mathbf{A}_f \Phi_f^{(p)})$. If one knows $\mathbf{e}_f^{(p)}$, the exact solution Φ_f can be obtained by simply adding $\mathbf{e}_f^{(p)}$ to $\Phi_f^{(p)}$. In order to get $\mathbf{e}_f^{(p)}$, one has only to solve the fine grid residual equation. Because this corresponds to solving the original fine grid equation, however, one solves coarse grid residual equation $\mathbf{A}_c \mathbf{e}_c^{(p)} = \mathbf{r}_c^{(p)}$ where coarse grid residual $\mathbf{r}_c^{(p)}$ is obtained from $\mathbf{r}_f^{(p)}$ by applying restriction operator $\mathbf{R}_{f \rightarrow c}$. Then, the coarse grid error, $\mathbf{e}_c^{(p)}$, is used for approximate estimation of $\mathbf{e}_f^{(p)}$ by using prolongation operator $\mathbf{P}_{c \rightarrow f}$ that converts $\mathbf{e}_c^{(p)}$ to $\mathbf{e}_f^{(p)}$. Correction of the intermediate fine grid solution $\Phi_f^{(p)}$ with the approximate $\mathbf{e}_f^{(p)}$ estimated from $\mathbf{e}_c^{(p)}$ is expected to eliminate effectively the low frequency errors of the fine grid solution, because they attenuate more effectively in coarse grid equation than in fine grid equation.

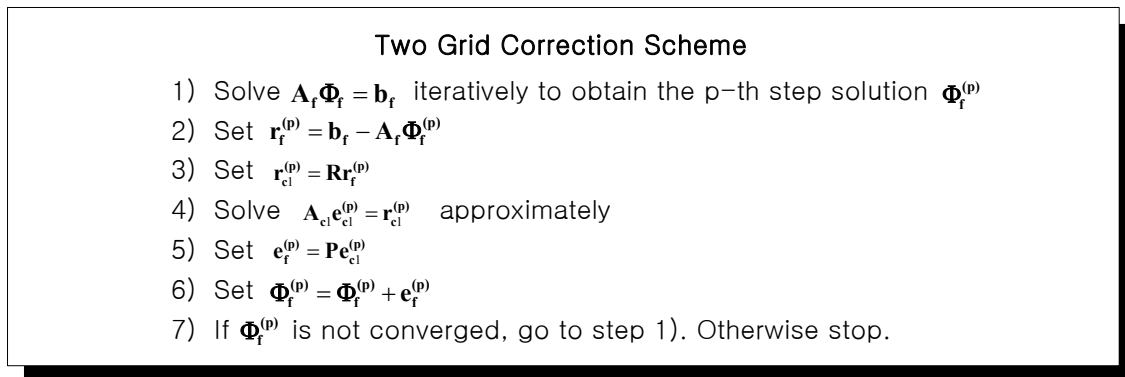


Figure 2. Algorithm of Two Grid Correction Scheme

The two-grid correction scheme described above can be recursively applied to the multigrid correction scheme by adopting V-cycle or W-cycle multigrid scheme, as shown in Fig. 3. Because the prolongation operator, Eq. (11), is dependent on fine grid solution that is the neutron flux in our calculation, we cannot correct the solution of $c1$ grid equation by using $c2$ grid residual equation. For the $c1$ grid solution is not neutron flux but the error of neutron flux and consequently the conventional V or W-cycle cannot be implemented with our prolongation

operator. So we devised the modified W-cycle that uses c2 grid residual equation to correct the fine grid solution directly, as illustrated in comparison with V or W-cycle in Fig. 3.

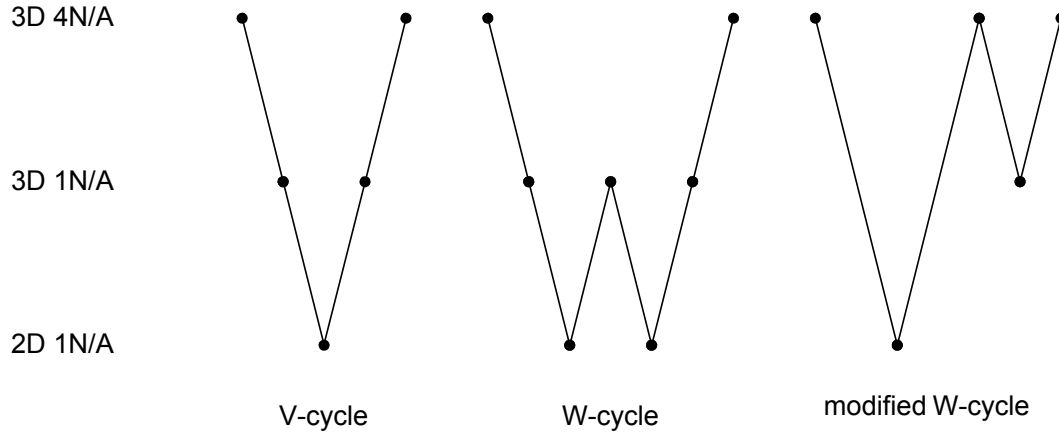


Figure 3. V-cycle, W-cycle, and modified W-cycle

2.4 Adaptive Time Step Size Control by Coarse Grid Equations

The adaptive time step size control method is designed to attain the desired fidelity of the transient solution and to reduce the computing time as well. The fully implicit temporal differencing scheme that we adopted here for the transient solution of the diffusion equation has the second-order derivative truncation error. Crouzet and Turinsky derived a second-order derivative truncation error-based adaptive time control method using the time step doubling technique[2], which is expressed by

$$\Delta t^{new} = \Delta t \times \sqrt{\frac{\varepsilon}{E_n}}. \quad (19)$$

ε is a user-provided constant corresponding to the desired accuracy. E_n is the estimated truncation error at the step n . For the difference scheme having the second-order derivative truncation error, it is obtained by

$$E_n = \Phi_n - \Phi_n^{\Delta t} \simeq -\frac{1}{3} \Delta \Phi_n^{\Delta t}; \quad \Delta \Phi_n^{\Delta t} = \Phi_n^{\Delta t} - \Phi_n^{2\Delta t} \quad (20)$$

where $\Phi_n^{\Delta t}$ and $\Phi_n^{2\Delta t}$ are the computed fluxes at time step n with the time step sizes of Δt and $2\Delta t$. Crouzet and Turinsky suggested solving the following linear equation for $\Delta \Phi_n^{\Delta t}$,

$$\mathbf{A}_n^{2\Delta t} \Delta \Phi_n^{\Delta t} = \boldsymbol{\delta}_n^{2\Delta t} \quad \text{with} \quad \boldsymbol{\delta}_n^{2\Delta t} = \mathbf{A}_n^{2\Delta t} \Phi_n^{\Delta t} - \mathbf{b}_n^{2\Delta t}. \quad (21)$$

$\mathbf{A}_n^{2\Delta t}$ and $\mathbf{b}_n^{2\Delta t}$ are the matrix and source vector, respectively, which define the transient equation for the time step n flux, $\Phi_n^{2\Delta t}$, with the step size of $2\Delta t$.

To achieve the adaptive time step size control, one has to solve Eq. (21). Because this corresponds to solve the temporal difference equation one more time at every time step, it is unavoidable to spend roughly 50 % of the computation overhead by the above method.

In order to reduce the computation overhead, we suggest using the coarse grid equations instead of the fine-grid equation that Crouzet and Turinsky used. The Multigrid correction scheme employs two coarse grid sizes of 3D 1N/A grid size and 2D 1N/A grid size. Using the restriction operator, one can readily obtain the coarse grid residual equation corresponding to Eq. (21) for each coarse grid size;

$$\mathbf{A}_{n,c1}^{2\Delta t} \Delta \Phi_{n,c1}^{\Delta t} = \delta_{n,c1}^{2\Delta t} \quad (22)$$

or

$$\mathbf{A}_{n,c2}^{2\Delta t} \Delta \Phi_{n,c2}^{\Delta t} = \delta_{n,c2}^{2\Delta t} \quad (23)$$

where

$$\delta_{n,c1}^{2\Delta t} = \mathbf{R}_{f \rightarrow c1} \delta_n^{2\Delta t} \quad (24)$$

and

$$\delta_{n,c2}^{2\Delta t} = \mathbf{R}_{c1 \rightarrow c2} \delta_{n,c1}^{2\Delta t} \quad (25)$$

Then one can solve Eq. (22) or Eq. (23) in much shorter computation time because the number of unknowns of these equations is much smaller than that of Eq. (21).

3. NUMERICAL RESULTS AND DISCUSSION

NEACRP PWR rod ejection benchmark A1 problem is chosen for the test of the computational efficiency of the temporal adaptive 3CGS. Fig. 4 shows the normalized transient core power calculations with three different constant time step sizes of 0.1ms, 0.5ms, and 2ms in comparison with the reference calculation with the very fine time step size of 0.01ms. The larger the time step size is, the larger the discrepancies between the reference and the coarse time step calculations are observed in peak power and peak time. This is because the per-step temporal truncation error is proportional to the square of the chosen time step size and accumulates to contribute to the net truncation error as the power transient progresses.

The adaptive time step size control requires the estimation of the truncation error at each time step. Because the step doubling method is the basis for this, we first examined its effectiveness by comparing in Fig. 5 the per-step truncation error estimated by Eq. (20) with the reference truncation error estimated by the difference between the reference solution for Eq. (4) with fine temporal step (0.01ms) and the single-step solution with the chosen time step (say, 0.1ms or 0.5ms). The initial conditions necessary for the step doubling method and the single step solution

here are taken from the fine step reference results as shown in Fig. 4. The results in Fig. 5 show that the per-step truncation error estimates by the step doubling method agree very well with the reference estimates when the temporal step size is as small as 0.1 or 0.5 ms. With the large temporal step size of 2 ms, however, some discrepancies are observed between two estimates.

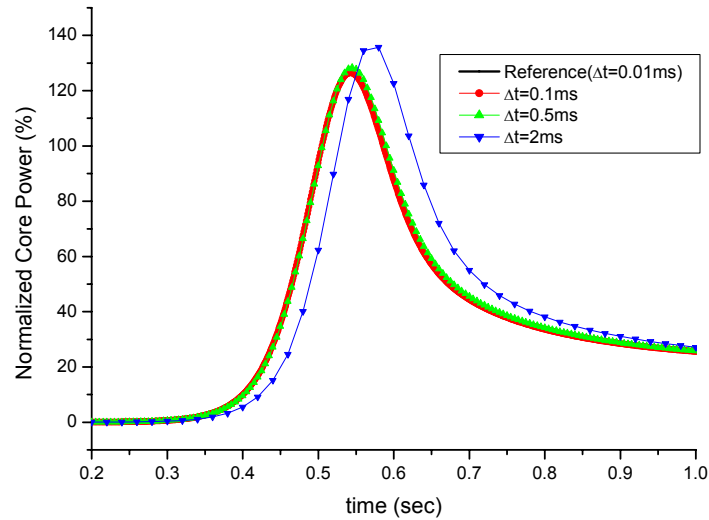


Figure 4. Normalized core power for constant time step size calculation

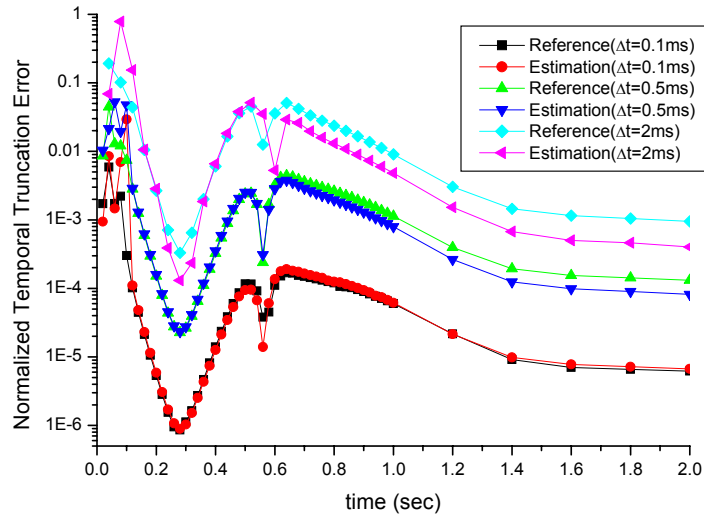


Figure 5. Temporal truncation errors for constant time step size calculation

As a way to reduce the additional computation time caused by the step-doubling calculations, we suggested using the coarse grid residual equations (22) and Eq. (23) instead of the fine grid

residual equation (21). Fig. 6 compares the per-step temporal truncation errors from the coarse and the fine grid residual equations.

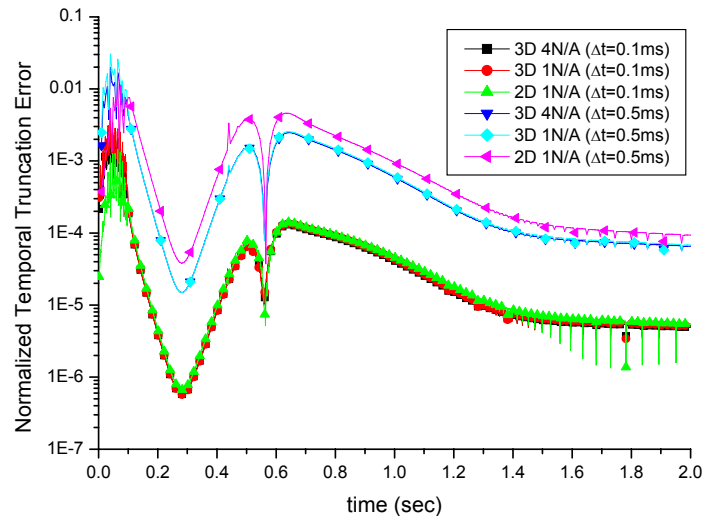


Figure 6. Temporal truncation errors from coarse grid based step-doubling method

The 3D 1N/A coarse grid residual equation (22) estimates almost the same temporal truncation errors as 3D 4N/A fine grid equation (21). The estimates by the 2D 1N/A coarse grid residual equation (23) are acceptably good. But they show some discrepancies from those with the 3D counterparts - especially when the temporal step size is as large as 0.5ms.

Because of the above result, the 3D 1N/A coarse grid residual equation, i.e., Eq. (22) is chosen as the basis of the truncation error estimate each step by the step-doubling method and variable time step size control for the transient calculations here. Fig. 7 shows the temporal adaptive 3GCS calculations for the NEACRP A1 benchmark problem with the variable time step size determined by user-specified temporal truncation error criteria ϵ . Tables I and II summarize some key transient parameters of the A1 problem that are obtained by constant time step size calculations and by variable time step size control calculations, respectively. Note that the constant time step calculations fall off the reference results on the peak power and time of the power peak when the time step is greater than 0.5ms. In contrast, the variable time step calculations agree well with the reference transient results for the truncation error criterion ranging from 0.0005 to 0.01. The CPU times for the transient calculations on PENTIUM4 1.8GHz PC show that the variable time step 3GCS calculations are fast and accurate. Besides, the overhead of the step doubling calculations is less than 20 % of the total calculation time by using coarse grid residual equation (22) for per-step truncation error estimates.

The most popular iterative solution method currently in use for the nodal neutron kinetics equations is the preconditioned BiCGSTAB. Table III shows a comparison of efficiencies of several BiCGSTAB methods with differing preconditioners and the 3GCS in terms of the CPU time taken for NEACRP A1 problem analysis. The time step size is adaptively adjusted with

temporal truncation error criterion of 0.001. All the methods predict the peak power and peak time very similarly. But the total CPU times differ from one method to another. The preconditioners speed up the BiCGSTAB calculation. Among preconditioners considered here, the BILU3D conditioner is the most efficient. The 3GCS is as efficient as the BiCGSTAB method with BILU3D preconditioner. The results of Table III indicate that both acceleration methods can reduce more than 70% of the CPU time of the non-acceleration method. The incorporation of the BILU3D preconditioner into the 3GCS improves further the efficiency of the multigrid method. In terms of the CPU time, roughly 40 % is saved in iterative solution process by incorporating the BILU3D preconditioner. In terms of the overall transient analysis time that includes nonlinear nodal solution time and thermal feedback calculation time for fuel temperature and coolant thermal-hydraulic properties, the 3GCS with BILU3D preconditioner is observed to reduce it by about a half.

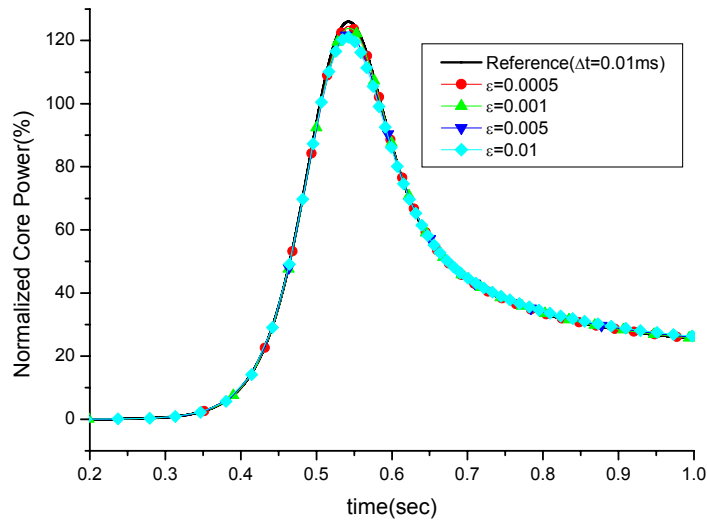


Figure 7. Normalized core power with variable time step size control method

Table I. Results of constant time step size calculation

Constant time step size (Δt)	0.01ms	0.1ms	0.5ms	2ms
Peak Power (%)	125.96	126.38	128.33	135.68
Peak Time (sec)	0.5425	0.5430	0.5450	0.5800
Total Time Steps	50000	5000	1000	250
Total Calculation Time (sec)	4902.2	488.2	114.9	35.5

Table II. Results of variable time step size control calculation

Temporal truncation error criterion(ϵ)	0.0005	0.001	0.005	0.01
Peak Power (%)	124.49	123.92	121.74	121.05
Peak Time (sec)	0.5431	0.544	0.5449	0.5426
Total Time Steps	959	490	187	121
Step-doubling Calculation Time (sec)	27.2	14.6	5.6	3.8
Total Calculation Time (sec)	151.6	83.6	35.9	25.2

Table III. Summary of results for preconditioned BiCGSTAB methods with or without multigrid correction scheme

Preconditioner	None	Jacobi	ILU	BILU3D	MG None	MG Jacobi	MG ILU	MG BILU3D
Peak Power (%)	123.87	123.87	123.91	123.95	123.86	123.86	123.86	123.92
Peak Time (sec)	0.544	0.544	0.543	0.543	0.544	0.544	0.544	0.544
Total Time Steps	490	490	490	489	490	490	489	490
Variable Time Step Size Calculation Time (sec)	15.6	15.6	14.6	15.5	14.4	14.7	14.6	14.6
Iteration Calculation Calculation Time (sec)	93.1	71.2	54.8	26.5	25.3	21.5	21.8	16.6
Total Calculation Time (sec)	162.9	140.2	128.3	93.9	94.4	90.0	95.4	83.6

5. CONCLUSIONS

In this paper a temporal adaptive 3GCS is presented for the transient nodal kinetics calculations. The 3GCS solves 3D 4N/A fine mesh nodal transient equations and two coarse mesh nodal equations corresponding to 3D 1N/A and 2D 1N/A spatial nodes on the modified W-cycle. The temporal step size for each time step is determined adaptively in accordance with the preset temporal truncation error criteria through the step-doubling calculations based on the 3D 1N/A coarse grid residual equation that is defined directly from 3GCS without any additional computational effort. Through the analysis of the NEACRP A1 benchmark problem, it is demonstrated that the step-doubling method based on coarse grid residual equation can reduce

the computation overload considerably, say, to less than 20% of the total calculation time. It is also demonstrated that, in terms of the CPU time, the 3GCS is about 2~4 times faster than the non-preconditioned or preconditioned BiCGSTAB iteration methods and the BILU3D-preconditioned 3GCS is the most efficient among the iteration schemes considered here. From these benchmark results, it is concluded that the temporal adaptive 3GCS employing the coarse grid residual equation for step size control provides a very efficient iterative solution scheme for transient nonlinear nodal calculations.

REFERENCES

1. Ku Y. Chung and Chang H. Kim, "A Three Grid Correction Scheme for Transient Nonlinear Nodal Calculation," *M&C 2001* Salt Lake City, Utah, USA, September 2001.
2. N. Crouzet and P. J. Turinski, "A Second-Derivative-Based Adaptive Time-Step Method for Spatial Kinetics Calculations," *Nucl. Sci. Eng.*, **123**, pp. 206-214 (1996).
3. H. G. Joo and T. J. Downer, "An Incomplete Domain Decomposition Preconditioning Method for Nonlinear Nodal Kinetics Calculations," *Nucl. Sci. Eng.*, **123**, pp. 403-414 (1996).
4. H. A. Van Der Vorst, "BI-CGSTAB: A fast and smoothly converging variant of BI-CG for the solution of nonsymmetric linear systems," *SIAM J. Sci. Stat. Comput.* **13**, pp. 631-644 (1992).
5. T. A. Taiwo, H. S. Khalil, J. E. Cahalan, and E. E. Moris, "Time-Step Selection Considerations in the Analysis of Reactor Transients with DIF3D-K," *Trans. Am. Nucl. Soc.*, **68**, pp. 429-430 (1993).
6. T. N. Sutton and B. N. Aviles, "Diffusion Theory Methods for Spatial Kinetics Calculations," *Progress in Nuclear Energy*, Vol. 30, No. 2, pp.119-182 (1996).
7. H. Finnemman, "NEACRP 3D LWR Core Transient Benchmark - Final Specifications," NEACRP-L-335(Revision 1) (1992).
8. H. G. Joo, Guobing Jiang, Douglas A. Barber and T. J. Downer, "PARCS: A Multi-dimensional Two-Group Reactor Kinetics Code Based on the Nonlinear Analytic Nodal Method," PU/NE-97-4, Purdue University (1997).
9. K. S. Smith, "Nodal Storage Reduction by Nonlinear Iteration," *Trans. Am. Nucl.* **44**, 265 (1983).
10. W. L. Briggs, *A Multigrid Tutorial*, SIAM, Philadelphia (1987).